J Mater Sci

Novel flexible, hybrid aerogels with vinyl- and methyltrimethoxysilane in the underlying silica structure

Telma Matias[1], Catarino Varino[1], Hermínio C. de Sousa[1], Mara E. M. Braga[1], António Portugal[1], Jorge F. J. Coelho[2], and Luisa Durães[1,*]

[1] CIEPQPF, Department of Chemical Engineering, University of Coimbra, Rua Sílvio Lima, 3030-790 Coimbra, Portugal
[2] CEMUC, Department of Chemical Engineering, University of Coimbra, Rua Sílvio Lima, 3030-790 Coimbra, Portugal

Received: 22 February 2016
Accepted: 8 April 2016

ABSTRACT

Flexible, monolithic and superhydrophobic silica aerogels were obtained by combining methyltrimethoxysilane (MTMS), vinyltrimethoxysilane (VTMS) and tetramethylorthosilicate (TMOS) (50:30:20 mol%) in a one-step base-catalyzed co-precursor sol–gel procedure. Polybutylacrylate (PBA) and polystyrene (PS) were grafted and cross-linked in the gel aiming to enhance the mechanical performance. Fourier transform infrared spectroscopy, thermogravimetry analysis and scanning electron microscopy confirmed the presence of the polymers as a binding coating on the 3D silica network, primarily formed by firmly connected 3–5 μm secondary particles. When compared to the MTMS-based aerogels, the VTMS–MTMS–TMOS-derived aerogels, either reinforced or not, show a threefold increase of the bulk density (to ~150–160 kg m^{-3}) and a consequent decrease in the surface area and average pore size; the thermal conductivity also increases to 60–70 mW m^{-1} K^{-1}, a 50 % increase over the values of MTMS-derived aerogels. Although these tendencies are more marked in the polymer-reinforced materials, the change of the silica skeleton from MTMS to VTMS–MTMS–TMOS is responsible for the main differences. The VTMS–MTMS–TMOS underlying structure gives a fourfold increase in compressive strength relatively to the MTMS-derived aerogels, even when not reinforced. In addition, it retains a high elongation at break (40–50 %) and flexibility—modulus of 25 kPa for the PBA-reinforced aerogel, the more flexible aerogel, and modulus of 91 kPa for PS-reinforced aerogel, the stiffer and stronger material. The obtained aerogels have touch feeling that resembles that of expanded polystyrene foams, and also show negligible particle shedding, which is a valued characteristic for aerospace applications.

Address correspondence to E-mail: luisa@eq.uc.pt

DOI 10.1007/s10853-016-9965-9

Published online: 21 April 2016

Introduction

Organically modified silica aerogels are materials with a three-dimensional nanostructure that present unique properties like very low thermal conductivity and density, high hydrophobicity, porosity and surface area, and, with some network modifications, an enhanced flexibility. Due to their thermal insulation performance and extremely low density, these materials have attracted special attention to Space engineering applications that involve thermal/acoustic/vibration protection, for example for atmosphere re-entry and Mars vehicles, satellite and spacecraft components, cryogenic tanks and space suits [1, 2]. Silica-based aerogels can also be used for many earthly applications such as building insulation, heat storage devices, catalyst supports, oxygen/humidity sensors, adsorbents for environmental clean-up, among others [3–8].

Despite their great potential for thermal insulation and, in some cases for presenting significant flexibility, organically modified silica aerogels still present poor mechanical strength which is mostly due to the inherent ceramic brittleness of the silica backbone. In the last years, some solutions have been proposed to improve the silica aerogels mechanical strength. These solutions include, for example, the use of organic polymers (polyacrylate, polyimide, epoxide, polystyrene and polyurea) to coat and/or cross-link the silica secondary particles, the inclusion of organic bridging groups in the silica backbone of the aerogels by using organic bridged bis-silanes (like 1,6-*bis*(trimethoxysilyl)hexane—BTMSH and 1,2-*bis*(trimethoxysilyl)ethane—BTMSE) and the dispersion of fibres on the sol during the synthesis [9–11].

Organic–inorganic aerogels, although thermally less stable and normally having higher density, offer a new range of possibilities in respect to their functionalities. The combination of the inorganic component properties with the organic ones allows to mitigate some of the drawbacks of the inorganic part. Vinyltrimethoxysilane (VTMS) is a silica precursor that offers the advantage of having three hydrolysable alkoxy groups, which allow the silica structure to grow, and one vinyl polymerisable group. This reactive functionality opens the possibility of further reactions with organic monomers and allows to produce hybrid aerogels with an oligomer component effectively linked to the silica structure, thus leading to covalently connected networks (class II hybrids) [10]. The limitation on the growth of the organic part due to the already formed inorganic structure will be a benefit aiming to control the density increase of the final material.

A few authors have already studied formulations with VTMS, using tetramethylorthosilicate (TMOS) as main precursor. Nguyen et al. [12] introduced styrene in a silica network obtained from TMOS, VTMS and BTMSH, in order to promote the polymerization with the vinyl groups and to improve the final elastic response of silica aerogels. Results revealed that some formulations of polymer cross-linked aerogels recovered completely their length after compression until a 25 % strain. Guo et al. [13] also used VTMS and TMOS precursors, but in this case the bridged bis-silane spacer was *bis*[3-(triethoxysilyl)propyl]disulfide (BTSPD) and no monomer was added. TMOS precursor was selected because it allows obtaining materials with high specific surface area and Young's modulus, whereas the purpose of using VTMS was only to enhance materials hydrophobicity and, finally, the addition of BTSPD was envisaged to increase the elastic recovery of the materials dimensions after compression. The optimal combination of these precursors allowed obtaining materials with almost full recovery after compression.

This work aims to develop novel hybrid silica aerogels, using the VTMS precursor to provide the vinyl polymerizable groups (–CH=CH_2) for the cross-linking of the silica skeleton with polymer, in order to reinforce the flexible aerogels obtained from methyltrimethoxysilane (MTMS) and to prevent the particle shedding from them. Several combinations and mole fractions of TMOS/MTMS/BTMSH precursors were tested with VTMS until reaching a formulation that gave rise to a monolithic and flexible material. After selecting the best organically modified silica (ormosil) formulation, the formation of hybrid aerogels was carried out by compounding them with styrene or butyl acrylate, followed by free radical polymerization induced by a curing process. The obtained hybrid gels were dried with supercritical CO_2, in order to retain their monolithicity and highly porous structure. The more promising aerogels in terms of monolithicity, flexibility and lightness were then subjected to further chemical, physical, thermal and mechanical characterization, being the results compared with the properties of the aerogels obtained from the MTMS precursor alone.

Experimental

Preliminary study

Selection of the best ormosil formulation

In order to build the silica network, modified with different organic functional groups, the selected precursors were (i) MTMS, because it allows to obtain monolithic, hydrophobic, very low density and flexible materials; (ii) VTMS, that provides the vinyl polymerizable groups; (iii) TMOS, due to its fast hydrolysis and condensation; (iv) BTMSH, since the spacing alkyl bridge allows to covalently reinforce the network and enlarge the pores of the silica structure.

Different combinations of the referred precursors were tested, varying their relative amount (TMOS, 12–75 mol%; MTMS, 30–80 mol%; VTMS, 18–50 mol%; BTMSH, 0–50 mol%). The considered selection criteria of the best ormosil formulation were the aerogels monolithicity, apparent flexibility and measured bulk density.

Selection of monomers/solvents for the aerogels reinforcement stage

Two polymers were selected for the aerogel reinforcement: polystyrene (PS), considering its regular application in thermal insulation, and polybutylacrylate (PBA), due to its low glass transition temperature (−49 °C) that widens the service temperature range of the final materials. It is worth noting that the glass transition temperature of PS is ~100 °C, which can be easily reached in the shell of Space devices/vehicles. Starting from styrene and butyl acrylate monomers and polymerizing them through free radical polymerization, both types of polymer-reinforced materials allowed to obtain monolithic, flexible and hydrophobic hybrid aerogels, and thus the corresponding samples were further characterized for comparison.

Initially, five solvents were considered, namely chlorobenzene (CBz), tetrahydrofuran (THF), chloroform, dimethylformamide (DMF) and dimethyl sulfoxide (DMSO). Pre-prepared ormosil gels were immersed in these solvents and the modifications observed in the gels allowed the selection of the most appropriate solvent to be used. THF and CBz were the selected solvents, as they were able to keep the monolithicity of the gels and, at the same time, to allow for the highest gel swelling. It is known that, in the case of enhanced gel swelling, the diffusion of the monomer/initiator in the porous structure is more effective.

Synthesis of the hybrid aerogels

VTMS ($H_2C{=}CHSi(OCH_3)_3$, 98 %, Aldrich), TMOS ($Si(OCH_3)_4$, 98 %, Fluka), MTMS ($CH_3Si(OCH_3)_3$, 98 %, Aldrich), BTMSH ($C_{12}H_{30}O_6Si_2$, >95 %, Cymit), methanol (MeOH, CH_3OH, 99.8 %, Sigma-Aldrich), ammonium hydroxide (NH_4OH, 28–30 % in H_2O, Fluka), styrene ($H_2C{=}CHC_6H_5$, 99 %, Sigma-Aldrich), butyl acrylate (BA, $H_2C{=}CHCOO(CH_2)_3CH_3$, 99 %, Aldrich), α,α′-Azoisobutyronitrile (AIBN, $(CH_3)_2C(CN)N{=}NC(CH_3)_2CN$, 98 %, Aldrich), tetrahydrofuran (THF, C_4H_8O, 99.9 %, Sigma-Aldrich), chlorobenzene (CBz, C_6H_5Cl, 99.8 %, Aldrich) chloroform ($CHCl_3$, 99 %, Aldrich), dimethylformamide (DMF, $HCON(CH_3)_2$, 99.8 %, Aldrich) and dimethyl sulfoxide (DMSO, $(CH_3)_2SO$, 99.7 %, Aldrich) were used as received.

The employed experimental procedure can be divided in three main steps: the synthesis of the ormosil gel by sol–gel technology, the radical polymerization/cross-linking that allows introducing the polymeric reinforcement in the gel structure and, finally, the gel drying stage.

The ormosil gel synthesis starts by diluting the precursors in methanol and stirring the obtained solution in an ethanol/dry ice bath (<0 °C). A previously prepared aqueous solution of ammonium hydroxide (1 M) is then added to the precursors solution. The resultant sol is later transferred into plastic syringes and aged for 2 days. In a second step, a solution containing AIBN (initiator), monomer (BA or styrene) and solvent (THF or CBz) is prepared taking into consideration the amount/volume of gel obtained in the first step. Gels are then soaked in this solution for 3 days, followed by a solvent exchange (replacing the solution by fresh THF) and a heat treatment for 24 h at 75 °C. After 24 h, the solvent was exchanged two more times and the final gels were dried in a supercritical fluid extraction system, by passing supercritical CO_2 at 50 °C and 200 bar through samples, and after washing them with a continuous flow of liquid methanol at the same *T*–*P* conditions.

The total concentration of silicon was 1.82 M and the water/silicon molar ratio was 7.8. For 100 mL of

solution, 1 mL of ammonium hydroxide was added. A 50 % (w/w) monomer solution in THF/CBz was used for the radical polymerization/cross-linking (for 100 mL of gel, 50 g of monomer and 50 g of solvent were used). The quantity of the initiator was 3 % of the weight of the employed monomer.

The synthesis was replicated three times for the most promising aerogel formulations.

Characterization

The samples taken for characterization were cut from several parts of the original monoliths, in order to increase reliability of the results. In the case of qualitative analyses, for each type of aerogel, the samples were taken from the monolith that exhibited a bulk density closest to the average value.

Fourier transform infrared (FTIR) transmission spectroscopy was performed on a *Jasco FTIR 4200* spectrometer. Spectra were collected using the KBr pellet method, the pellets being prepared with 80 mg of KBr and 0.2–0.3 mg of each aerogel. Wave number ranged from 400 to 4000 cm^{-1}, applying a resolution of 4 cm^{-1}.

Contact angle measurements, with Milli-Q water droplets, were conducted in a *Dataphysics model OCA 20* apparatus, at room temperature and using the sessile drop method, in order to conclude about the hydrophobicity of the aerogels.

Helium pycnometry (*Accupyc 1330, Micromeritics*) was used to measure the skeletal density (ρ_s) of the aerogels which along with the bulk density (ρ_b) allowed to evaluate the porosity of the samples (Eq. 1). The bulk density was obtained by the measurement of mass and volume of aerogel pieces.

$$\text{Porosity}(\%) = ((1/\rho_b) - (1/\rho_s))/(1/\rho_b) \times 100. \quad (1)$$

Nitrogen gas adsorption on the samples was performed in an *Autosorb iQMP* equipment, from *Quantachrome Instruments*, after desorption of impurities during 3 days at 50 °C in a vacuum oven, followed by degassing in the equipment at 80 °C. Surface area (A_{BET}) was evaluated applying the BET theory to the data in the relative pressure interval 0.05–0.25 of the N_2 adsorption isotherm taken at 77 K. The average pore sizes were estimated by the simple models specified in Eqs. 2 and 3, which often apply to polymer-reinforced aerogels exhibiting a highly constrained network [14].

$$\text{Pore volume}, V_p = (1/\rho_b) - (1/\rho_s), \quad (2)$$

$$\text{Average pore diameter} = (4V_p)/A_{BET}. \quad (3)$$

SEM micrographs were taken on a *JEOL JMS-5310* Scanning Electron Microscope in order to observe the surface microstructure of the aerogels. The samples were coated with a layer of vapour-deposited Au, because prepared aerogels presented high electrical resistivity.

Thermal conductivity was evaluated from data collected with a *Hot Disk Thermal Constants Analyser*, model *TPS2500*, at 20 °C. This equipment has reproducibility better than 1 % and accuracy better than 5 %.

A Simultaneous Differential Scanning Calorimeter (DSC/TGA), model *SDT Q500*, from *TA Instruments*, was used to study the thermal stability of the aerogel samples and to compare the mass loss in samples with/without polymer, in order to estimate the amount of polymer incorporated in the reinforced aerogel. Samples were placed in an alumina pan and heated from room temperature up to 1200 °C, at a constant rate of 10 °C min^{-1} and under a nitrogen flow.

Compression tests were performed using a *Shimadzu AG-IS 100KN* device equipped to control the compression velocity and a *AND EK-1200i* balance. Cylindrical aerogel samples were used, with a diameter in the range 15–17 mm and a length of 20–23 mm. The data collected for each test were converted into a stress–strain curve. Young's modulus, compression strength and elongation at break were obtained from these curves.

Results and discussion

Best ormosil formulation

The prepared aerogels were evaluated in terms of bulk density and monolithicity, as well as for their flexibility when handled. Regarding bis-silanes, it is known that their alkyl chains originate more flexible aerogels when combined with TMOS, i.e. when included in rigid and brittle native silica aerogels [12]. In the case of MTMS-derived aerogels, the silica skeleton is already highly disordered and flexible [15], thus the incorporation of a bis-silane tends to induce more organization and stiffness into the silica structure, which lead to higher bulk density, even with small added amounts of BTMSH [16]. In the

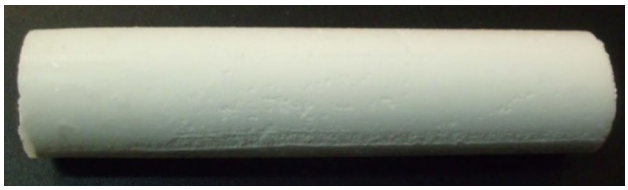

Figure 1 Aerogel obtained from 30 % VTMS, 50 % MTMS and 20 % TMOS.

current work, this was also observed and led to the rejection of formulations that contained in their composition the precursor BTMSH.

The selected ormosil formulation was prepared from 30 mol% VTMS, 50 mol% MTMS and 20 mol% TMOS (Fig. 1). When prepared without the polymeric reinforcement, the obtained aerogel already presents very good integrity and flexibility (low Young's modulus).

Selected monomers and solvents for the aerogels reinforcement stage

In a second step, four types of samples of cross-linked hybrid aerogels were prepared, using two monomers—styrene and BA—and two solvents—THF and CBz. The aerogels prepared with CBz/styrene and CBz/BA were excluded due to their fragility and lack of flexibility—they easily crumble up by simple handling; in the case of CBz/BA, the resultant aerogel was not even monolithic (Fig. 2a, b) [17]. In fact, according to supplier data and open literature [18], CBz is a denser and viscous solvent when compared with THF, and this fact could hamper the diffusion of monomers and, consequently, the polymerization process.

Therefore, only the aerogels prepared with THF and styrene/BA in the polymerization/cross-linking step were used for further chemical, physical, thermal and mechanical characterization.

In order to study and compare the effect of the styrene and BA polymerization/cross-linking, the correspondent ormosil aerogel (non-reinforced) was also fully characterized. Furthermore, some of the key properties of these three samples were also compared with an aerogel obtained with MTMS precursor alone, which was synthesized through the experimental procedures described in a previous work [15] and was dried in a supercritical fluid (CO_2) extraction system (using the same procedures described in this work). Table 1 summarizes all the samples that will be referred in the remaining part of this text.

Chemical structure of the materials

The FTIR spectra of reinforced and non-reinforced aerogels with MTMS–VTMS–TMOS in the underlying structure are presented in Fig. 3. The chemical bonds vibrations that gave rise to the IR absorption bands of the spectra are also indexed in Fig. 3, according to the typical vibrations data in the open literature [19, 20].

The three presented spectra suggest a chemical structure with similar silica backbone, showing the existence of an organically modified silica network that resulted from the sol–gel inorganic polymerization. Indeed, the absorption peaks at ~770, 1000 and 1100 cm^{-1} are ascribed to the stretching vibrations of Si–O–Si bonds, and the peak at ~440 cm^{-1} corresponds to the bending vibration of the same bonds, all appearing in the three spectra. The hydrophobicity of the aerogels is proven by the presence of methyl groups, which originates stretching vibrations of the C–H bonds that are found between 2800 and 3000 cm^{-1}, and the stretching vibrations of the Si–C bonds near ~850 cm^{-1}. The deformation vibrations of C–H bonds are also observed at ~1270 and

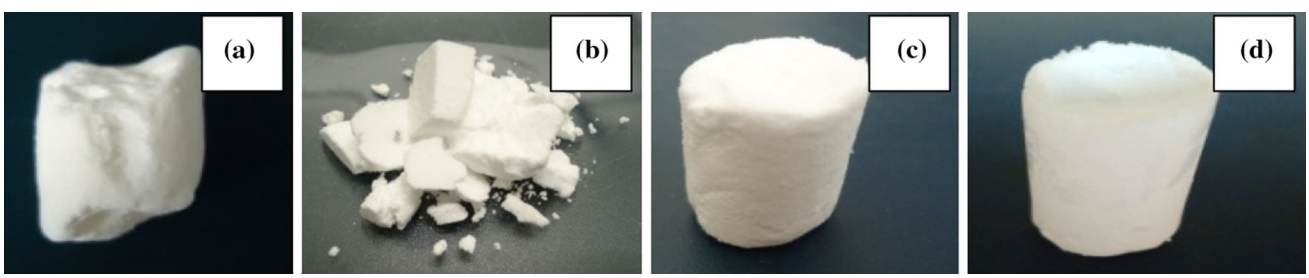

Figure 2 Aspect of the polymer-reinforced aerogels when using **a** CBz/styrene, **b** CBz/BA, **c** THF/styrene, **d** THF/BA.

Table 1 Summary of the samples that will be characterized and compared in the remaining sections

Sample	Sol–gel synthesis procedure	Silica precursors	Reinforcement
Non-reinforced aerogel	One-step, base catalyzed	MTMS–VTMS–TMOS	–
PBA-reinforced aerogel	One-step, base catalyzed	MTMS–VTMS–TMOS	PBA
PS-reinforced aerogel	One-step, base catalyzed	MTMS–VTMS–TMOS	PS
MTMS-derived aerogel	Two-step, acid–base catalyzed [15]	MTMS	–

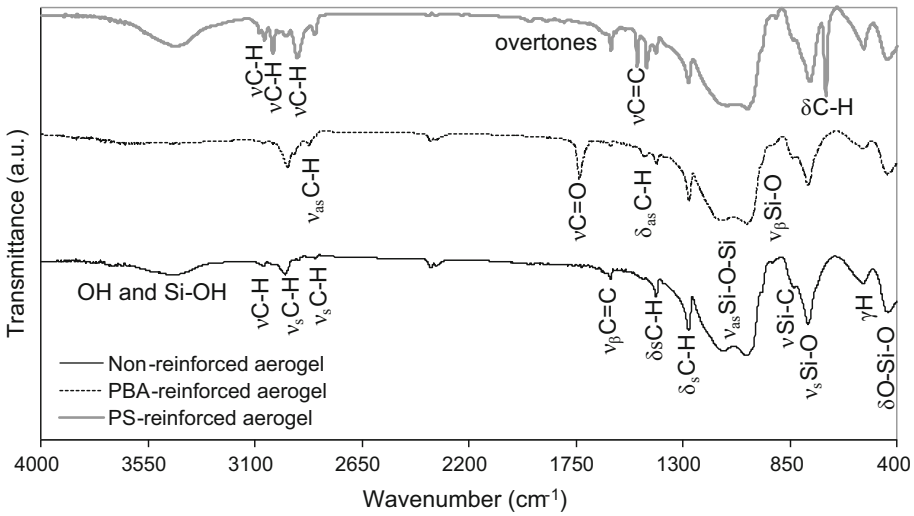

Figure 3 FTIR spectra for the prepared silica-based aerogels (ν—stretching vibration; δ—deformation vibration; γ—out-of-plane deformation vibration; *s*—symmetric; *as*—asymmetric; β—in-plane).

$\sim$1400 cm^{-1}, respectively. The above-described peaks are coincident with those already reported for a MTMS-derived aerogel structure [15].

It is worth to note that the three spectra of Fig. 3 also show peaks that correspond to vinyl groups (–CH=CH$_2$), at 542, 1413 and 1605 cm^{-1}, being the two first due to the bending vibrations of C–H bonds and the third due to the stretching vibration of the C=C bond. A small peak just above 3000 cm^{-1} is also visible, originated by the stretching vibration of =C–H. This fact means that the vinyl groups of VTMS did not react completely with the monomers/oligomers during polymerization, and some amount of unreacted monomers may be also present. This observation can be explained by hindered diffusion caused by the intricacy of the porous network; in fact, the aerogels porous structure is highly branched, with pores with multiple sizes and dead-ends, and the CH$_3$ groups from MTMS cause steric hindrance, which limit the connection of the BA/styrene monomers with inner vinyl groups. Moreover, premature termination of the polymerization process may occur by disproportionation and/or chain transfer, or simply by lack of space inside the pores.

The characteristic absorption band of C=O group stretching vibration from BA appears at 1736 cm^{-1} in the spectrum of the PBA-reinforced aerogel and this is the main difference between this sample and the other samples, suggesting the presence of linked polymer/oligomer in the silica skeleton of the reinforced aerogels. As the gel is washed with a continuous flow of methanol before drying, it very unlikely that this sharp peak could be only due to detached monomer in the system.

The presence of the aromatic ring in the PS-reinforced aerogel spectrum is noticeable by the peaks at 698, 1493, 3000 and 3081 cm^{-1}, which can be ascribed to the bending vibrations of C–H, the stretching vibrations of C=C and the stretching vibrations of C–H, respectively, all in the ring. The overtones found between 1600 and 2000 cm^{-1} are also characteristic of the presence of the aromatic ring.

Density and porous structure of the aerogels

The bulk density values of the non-reinforced and PBA-reinforced aerogels are very close, considering their uncertainty, but the PS-reinforced aerogel presents a higher value (Table 2). Still, both polymers lead to an increase of bulk density, in average, relatively to the non-reinforced aerogel, as the formed polymer and cross-linking will partially fill the pores

Table 2 Bulk density, porosity, specific surface area, average pore size, contact angle and thermal conductivity of non-reinforced and polymer-reinforced aerogels obtained with VTMS–MTMS–TMOS system; comparison with the MTMS-derived aerogel

Sample	Bulk density, ρ_b (kg m^{-3})	Porosity (%)	BET surface area, A_{BET} (m^2 g^{-1})	Average pore diameter[a] (nm)	Contact angle (°)	Thermal conductivity at 20 °C (W m^{-1} K^{-1})
Non-reinforced aerogel	150.9 ± 12.8	89	188.3 ($R^2 = 0.9992$)	125	150 ± 14	0.062 ± 0.004
PBA-reinforced aerogel	154.9 ± 7.8	89	–[b]	–	150 ± 6	0.060 ± 0.005
PS-reinforced aerogel	163.1 ± 11.7	88	222.7 ($R^2 = 0.9999$)	96	146 ± 6	0.072 ± 0.001
MTMS-derived aerogel	59.4 ± 5.2	94	365.9 ($R^2 = 0.9991$)	173	146 ± 3	0.038 ± 0.000

[a] Using Eqs. 2 and 3: includes all pore sizes

[b] It was not possible to obtain a reliable value (>10 m^2 s^{-1}) due to the highly constrained porous network

of the silica structure. The porosity presents values of 88–89 % (Table 2), which are higher than the values obtained by Nguyen et al. [12] for PS-reinforced silica aerogels, without using MTMS. Accordingly, the densities of VTMS–MTMS–TMOS-derived aerogels reported here, with or without polymeric reinforcement, are lower than the generality of values obtained in Ref. [12] or for other reinforced silica aerogels based in orthosilicates [10]. However, and as expected, the porosities found with this underlying silica structure are lower than the estimated for pure MTMS-derived materials, since the presence of TMOS tends to make denser aerogels.

As observed in Table 2, the BET specific surface area of the VTMS–MTMS-TMOS-derived aerogel without polymeric reinforcement is half of that obtained for MTMS-based aerogel, which is in good agreement with the bulk density and porosity values. The reinforcement with PS slightly increases the surface area when compared to the non-reinforced counterpart. This fact may be due to the rigid nature of the aromatic ring, which inhibits the closing of the pores/shrinkage of the silica structure [21, 22]. Nevertheless, it is possible to observe simultaneously the narrowing of the pores caused by the covering of secondary particles with the forming polymer. On the other hand, PBA is a more flexible polymer and, thus, more prone to adapt to the pores surface and cause the blocking of the pores entrance, which has complicated significantly the measuring of the N_2 adsorption isotherms. In fact, the BET area was always lower than 10 m^2 g^{-1} for the PBA-reinforced aerogel, which is not an expected result taking into account that this aerogel is not much different from the PS-reinforced aerogel in terms of the other structural properties.

Hydrophobicity and insulation characteristics

The water contact angle values obtained for the non-reinforced, for PBA-reinforced, for PS-reinforced aerogels and for the MTMS-derived aerogels, confirmed the highly hydrophobic nature of the obtained hybrid aerogel monoliths (Table 2). The VTMS and MTMS precursors are expected to be the main contributors to this hydrophobicity due to the presence of non-polar organic groups (vinyl and methyl) in the silica network. According to the obtained values, the introduction of the non-polar polymer/oligomer chains did not cause a significant change in the contact angle, possibly because the value was already extremely high.

The measurement of the thermal conductivity allows the evaluation of the suitability of the obtained hybrid aerogels for thermal insulation purposes. The results presented in Table 2 reveal a non-significant variation between the thermal conductivities of the non-reinforced and of PBA-reinforced aerogels synthesized with VTMS–MTMS–TMOS precursor system. However, the thermal conductivity of PS-reinforced aerogels was slightly increased when compared with the other two materials, which is certainly related to the higher bulk density (less porosity) of the PS-containing samples. Nevertheless, it can be concluded that the polymer incorporation

and cross-linking has no deleterious effect on the thermal insulation performance of the aerogels in the system here studied. Comparing with the result obtained for the MTMS-derived aerogel, the thermal conductivity values in the aerogels prepared from the VTMS–MTMS–TMOS system do not even double. The VTMS–MTMS–TMOS system (reinforced or non-reinforced) used in this work leads to higher thermal conductivities when compared to PS- and PBA-reinforced silica aerogels derived from pure TMOS [23], which gave values in the range 35–42 mW m^{-1} K^{-1}, although with similar values of bulk density. This is due to the large average pore sizes of our aerogels (in the range macropores) that enhance the thermal transport through the gas phase inside the pores.

Microstructure

Figure 4 shows the SEM images for the non-reinforced and polymer-reinforced aerogels, at magnifications of ×1000 a, c and e and ×5000 b, d and f.

Samples do not show noticeable differences in terms of the microstructure morphology of the 3D silica network, being the structural units small (3–5 μm) and spherical, with relatively uniform size. When polymers are incorporated into the silica backbone, the shape of the structural units becomes less defined and these are connected by larger necks, showing clearly the binding effect of the organic cross-linking (particularly noticed in Fig. 4d). If compared to the highly branched and sponge-like

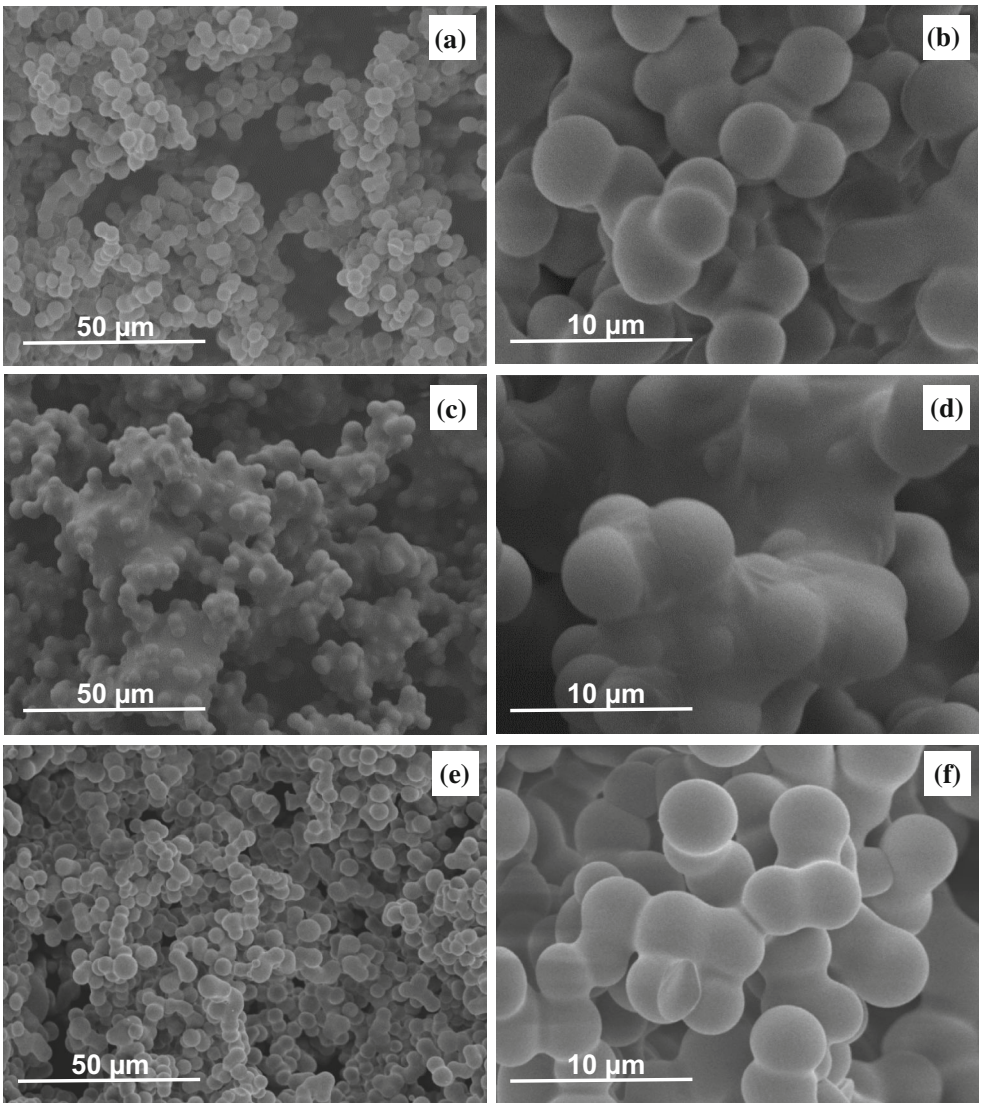

Figure 4 SEM images of **a, b** non-reinforced aerogel, **c, d** PBA-reinforced aerogel, **e, f** PS-reinforced aerogel.

structure of the MTMS-derived aerogels (as can be observed in Ref. [15]), the aerogels networks of Fig. 4 have much larger secondary particles, due to the enhancement of condensation reactions resulting from the use of TMOS precursor, which originates four siloxane bonds per silicon.

Thermal characterization

The thermal analysis allowed to conclude that the polymer-reinforced aerogels presented a higher weight loss than the non-reinforced aerogel (Table 3). Below 400 °C, in addition to the removal of impurities (solvent residuals, unreacted monomers/precursors) and of OH structural groups and to the thermal decomposition of vinyl groups that occur in all samples, it is clear that the thermal decomposition of the polymer/oligomer occurs in the case of the polymer-reinforced aerogels. PS and PBA have characteristic thermal degradation temperatures near 250 °C and 300 °C [24, 25]; however, in this work, the onset temperatures of these degradations are 50–100 °C shifted to higher temperatures, confirming the effective link of the polymer/oligomer to the silica porous structure, which increases the thermal stability of the grafted polymer due to the aerogel insulation behaviour.

By the difference in the weight losses, the relative weights (%) of incorporated PBA and PS in the reinforced aerogels could be estimated as ~10 and ~20 %, respectively. For temperatures above 500 °C, the thermal decomposition (in a non-oxidizing atmosphere) of the methyl groups provided by MTMS occurs in two stages, as previously discussed in an earlier work [2]. The higher size and molecular weight of the BA monomer, when compared to styrene, may explain the less effective diffusion process of BA in the porous network. The observed relative amounts of PBA and PS incorporated into the aerogels can also justify the obtained bulk density and thermal conductivity values that were discussed before.

Mechanical characterization

Compression tests were run on the prepared aerogels to study the effect of incorporating an organic reinforcement phase into the silica skeleton. The obtained results (Table 4) show that the PBA-reinforced aerogel is more flexible than the non-reinforced and PS-reinforced aerogels, because it presents the lowest value for the Young's modulus. On the contrary, the PS-reinforced aerogel is the more stiff material. These results can be easily understood considering the typical mechanical properties of PBA and PS homopolymers. However, when comparing the aerogels with VTMS–MTMS–TMOS in the underlying structure with the MTMS-derived aerogel, it is noticed that the later is a much more flexible material (Young's modulus of only 8.3 kPa). As TMOS makes the materials more rigid and brittle, it leads to the observed increase in the Young's modulus results.

Nguyen et al. [12] found Young's modulus values from hundreds of kPa to tens of MPa for the PS-reinforced TMOS–VTMS–BTMSH formulations, which lead to aerogels at least ten times more rigid than the

Table 3 Thermal analysis of non-reinforced and polymer-reinforced aerogels obtained with VTMS–MTMS–TMOS precursor system

Aerogel	Weight loss (%)	T_{onset} (°C)	T_{end} (°C)	Phenomena
Non-reinforced aerogel	1.5	278.3	395.9	Removal of adsorbed impurities and structural OH; decomposition of vinyl groups
	5.3	516.3	614.3	First stage of thermal decomposition of methyl groups
	2.8	716.3	819.3	Second stage of thermal decomposition of methyl groups
PBA-reinforced aerogel	14.1	342.0	411.2	Decomposition of PBA and remaining vinyl groups; removal of adsorbed impurities and structural OH
	5.3	501.5	611.1	First stage of thermal decomposition of methyl groups
	2.3	733.4	811.3	Second stage of thermal decomposition of methyl groups
PS-reinforced aerogel	26.1	376.5	431.5	Decomposition of PS and remaining vinyl groups; removal of adsorbed impurities and structural OH
	4.3	529.5	600.6	First stage of thermal decomposition of methyl groups
	2.4	726.3	812.4	Second stage of thermal decomposition of methyl groups

Table 4 Mechanical properties of non-reinforced and polymer-reinforced aerogels obtained with VTMS–MTMS–TMOS system and comparison with the properties of the MTMS-derived aerogel

Sample	Young's modulus (kPa)	Elongation at break (%)	Compression strength (kPa)
Non-reinforced aerogel	57	38	64
PBA-reinforced aerogel	25	42	66
PS-reinforced aerogel	91	52	68
MTMS-derived aerogel	8.3	68	17

ones prepared in this work. Thus, the aerogels here prepared are more prone to adapt to curved surfaces. Maleki et al. [23] obtained a modulus of 50–60 kPa for PS- and PBA-reinforced TMOS-derived aerogels (for the same time of polymerization), via surface-initiated Reversible Addition-Fragmentation Chain Transfer (RAFT) polymerization, which is a more complex chemical process, although more controllable. Nonetheless, the modulus value still is the double of the one achieved for the PBA-reinforced aerogel of this work.

As expected, in general, the elongation at break follows the opposite trend of the Young's modulus (Table 4), except for the case of the PS-reinforced aerogel that exhibits the highest value of both properties. Its higher elongation at break, while being the more rigid material, can be explained by the high amount of PS that was incorporated into the structure (as confirmed by thermal analysis). The lowest elongation at break is observed for the non-reinforced VTMS–MTMS–TMOS-derived aerogel.

The polymer-reinforced aerogels have higher compression strengths when compared to the non-reinforced counterpart. Since the found values for the polymer-reinforced and non-reinforced aerogels are close (Table 4), their increase in strength in relation to the MTMS-derived aerogel (~4×) is mainly due to the presence of TMOS and VTMS in the formulation. This fact turns the VTMS–MTMS–TMOS-derived aerogels easier to handle without breaking. Moreover, PBA seems to have an interesting effect in the elastic behaviour of the aerogels, as it allows to partially recover the flexible behaviour in relation to MTMS-derived aerogel. Very promising mechanical reinforcing results were also obtained by He et al. [26], who reinforced MTMS-derived aerogel-like materials by growing the silica network inside polyurethane sponges; values of stress in the interval 100–150 kPa were obtained at 50 % strain. However, the developed matrix is a composite, being the silica phase only in the pores of the sponge, and these mechanical properties are mainly afforded by the polyurethane scaffold.

Finally, due to the binding effect of the polymer in the secondary silica particles, the polymer-reinforced aerogels present negligible particle shedding, which is a crucial issue in the case of thermal insulation of devices/vehicles used in Space missions.

Conclusions

Monolithic and flexible, hybrid silica aerogels were synthesized using the precursor system VTMS–MTMS–TMOS, without and with polymeric reinforcement. PBA and PS were the tested polymeric reinforcing agents, and an optimized precursor formulation was achieved with the following molar ratios of co-precursors VTMS:MTMS:TMOS = 0.3:0.5:0.2.

FTIR and TG analyses confirmed the presence of the incorporated polymers into the aerogel structure, although part of the vinyl groups did not react most probably due to diffusional limitations (complex/ramified porous network; steric hindrance) and early termination of the polymerization process. The 3D silica network observed by SEM has micrometre-sized secondary particles (3–5 μm), which are much larger than the nanometre-sized particles obtained when MTMS is the sole precursor [15]. Moreover, the polymeric reinforcement seems to be visible in the microstructure of the reinforced aerogels, as a binding coating on these secondary particles.

The non-reinforced or the polymer-reinforced VTMS–MTMS–TMOS-derived aerogels show a threefold increase of the bulk density, accompanied by a significant decrease in the surface area and in the average pore size, when compared to the MTMS-based aerogels. These trends are clearer for the reinforced aerogels, but the main differences should be mostly due to the change of the silica backbone from MTMS to VTMS–MTMS–TMOS. This change also

produces an increase of the thermal conductivity from ~40 up to 60 mW m^{-1} K^{-1}. All the synthesized hybrid aerogels are hydrophobic, reaching the superhydrophobicity level (150°). In terms of the obtained mechanical properties, the aerogels produced from the VTMS–MTMS–TMOS system show fourfold higher compressive strengths if compared to the MTMS system, while maintaining a high elongation at break (40–50 %). Their flexibility is relatively high, from a modulus of 25 kPa for the PBA-reinforced aerogel to a modulus of 91 kPa for the PS-reinforced aerogel, the stiffer and stronger material here obtained.

Acknowledgements

This work was funded by FEDER funds through the Operational Programme for Competitiveness Factors—COMPETE and National Funds, through FCT—Foundation for Science and Technology under the projects PTDC/EQU–EPR/099998/2008—GelSpace—Silica-based Aerogels for Insulation of Spatial Devices, PEst-C/EQB/UI102/2011 and PEst-C/EQB/UI102/2013. Mara Braga acknowledges FCT for the fellowship SFRH/BPD/101048/2014 and for *Programa Ciência* 2008. The authors also acknowledge Active Aerogels for collaborating in this work.

References

[1] Durães L, Ochoa M, Portugal A, Duarte N, Dias JP, Rocha N, Hernandez J (2010) Tailored silica based xerogels and aerogels for insulation in space environments. Adv Sci Technol 63:41–46

[2] Ochoa M, Durães L, Beja AM, Portugal A (2012) Study of the suitability of silica based xerogels synthesized using ethyltrimethoxysilane and/or methyltrimethoxysilane precursors for aerospace applications. J Sol-Gel Sci Technol 61(1):151–160

[3] Koebel M, Rigacci A, Achard P (2012) Aerogel-based thermal superinsulation: an overview. J Sol-Gel Sci Technol 63(3):315–339

[4] Cuce E, Cuce PM, Wood CJ, Riffat SB (2014) Toward aerogel based thermal superinsulation in buildings: a comprehensive review. Renew Sustain Energy Rev 34:273–299

[5] Gibiat V, Lefeuvre O, Woignier T, Pelous J, Phalippou J (1995) Acoustic properties and potential applications of silica aerogels. J Sol-Gel Sci Technol 186:244–255

[6] Ward DA, Ko EI (1995) Preparing Catalytic Materials by the Sol-Gel Method. Ind Eng Chem Res 34(2):421–433

[7] Wang D, Liu Y, Hu Z, Hong C, Pan C (2005) Michael addition polymerizations of trifunctional amines with diacrylamides. Polymer 46:3507–3514

[8] Perdigoto MLN, Martins RC, Rocha N, Quina MJ, Gando-Ferreira L, Patrício R, Durães L (2012) Application of hydrophobic silica based aerogels and xerogels for removal of toxic organic compounds from aqueous solutions. J Colloid Interface Sci 380:134–140

[9] Aegerter MA, Leventis N, Koebel MM (2001) Aerogels handbook. Springer, New York

[10] Maleki H, Durães L, Portugal A (2014) An overview on silica aerogels synthesis and different mechanical reinforcing strategies. J Non-Cryst Solids 385:55–74

[11] Active Aerogels & University of Coimbra (Inventors: Ochoa M, Durães L, Perdigoto M, Portugal A) Flexible panels of hydrophobic aerogel reinforced with fibre felts. Patent WO 2015/016739 A2

[12] Nguyen BN, Meador MAB, Tousley ME, Shonkwiler B, McCorkle L, Scheiman DA, Palczer A (2009) Tailoring elastic properties of silica aerogels crosslinked with polystyrene. ACS Appl Mater Interfaces 1(3):621–630

[13] Guo H, Nguyen BN, McCorkle LS, Shonkwiler B, Meador MAB (2009) Elastic low density aerogels derived from bis[3-(triethoxysilyl)propyl]disulfide, tetramethylorthosilicate and vinyltrimethoxysilane via a two-step process. J Mater Chem 19(47):9054–9062

[14] Maleki H, Durães L, Portugal A (2015) Development of mechanically strong ambient pressure dried silica aerogels with optimized properties. J Phys Chem C 119(14):7689–7703

[15] Durães L, Ochoa M, Rocha N, Patrício R, Duarte N, Redondo V, Portugal A (2012) Effect of the drying conditions on the microstructure of silica based xerogels and aerogels. J Nanosci Nanotechnol 12(8):6828–6834

[16] Durães L, Maia A, Portugal A (2015) Effect of additives on the properties of silica based aerogels synthesized from methyltrimethoxysilane (MTMS). J Supercrit Fluids 106:85–92

[17] Varino C (2012) Synthesis of silica based hybrid aerogels using vinyltrimethoxysilane precursor. MSc dissertation, University of Coimbra

[18] Haynes WM (2015) CRC handbook of chemistry and physics, 96th edn. CRC Press, Boca Raton

[19] Al-Oweini R, El-Rassy H (2009) Synthesis and characterization by FTIR spectroscopy of silica aerogels prepared using several $Si(OR)_4$ and $R''Si(OR')_3$ precursors. J Mol Struct 919:140–145

[20] Becker HGO, Berger W, Domschke G, Fanghänel E, Faust J, Fischer M, Gentz F, Gewald K, Gluch R, Mayer R, Müller K, Pavel D, Schmidt H, Schollberg K, Schwetlick K, Seiler E, Zeppenfeld G (1997) Organikum, 2nd edn. Calouste Gulbenkian Foundation, Lisbon

[21] Maleki H, Durães L, Portugal A (2014) Synthesis of lightweight polymer reinforced silica aerogels with improved mechanical and thermal insulation properties for space applications. Micropor Mesopor Mater 197:116–129

[22] Loy DA, Jamison GM, Baugher BM, Myers AS, Assink RA, Shea KJ (1996) Sol–gel synthesis of hybrid organic–inorganic materials. Hexylene- and phenylene-bridged polysiloxanes. Chem Mater 8:656–663

[23] Maleki H, Durães L, Portugal A (2015) Synthesis of mechanically reinforced silica aerogels via surface-initiated reversible addition-fragmentation chain transfer (RAFT) polymerization. J Mater Chem A 3:1594–1600

[24] Peterson JD, Vyazovkin S, Wight CA (2001) Kinetics of the thermal and thermo-oxidative degradation of polystyrene, polyethylene and polypropylene. Macromol Chem Phys 202:775–784

[25] Hu Y-H, Chen C-Y, Wang C-C (2004) Thermal degradation kinetics of poly(*n*-butyl acrylate) initiated by lactams and thiols. Polym Degrad Stabil 84:505–514

[26] Coelho JFJ, Silva AMFP, Popov AV, Perlec V, Abreu MV, Gonçalves PMOF, Gil MH (2006) Single electron transfer-degenerative chain transfer living radical polymerization of N-butyl acrylate catalyzed by $Na_2S_2O_4$ in water media. J Polym Sci A 44:2809–2825